Current Spreading in Long Objects

REPORT DOCUMENTATION PAGE

1. REPORT DATE (DD-MM-YYYY)	2. REPORT TYPE	3. DATES COVERED (From - To)
October 2008	Technical	

4. TITLE AND SUBTITLE	5a. CONTRACT NUMBER
Current Spreading in Long Objects	5b. GRANT NUMBER
	5c. PROGRAM ELEMENT NUMBER

6. AUTHOR(S)	5d. PROJECT NUMBER
	13089022
D. Eardley	5e. TASK NUMBER
	PS
	5f. WORK UNIT NUMBER

7. PERFORMING ORGANIZATION NAME(S) AND ADDRESS(ES)	8. PERFORMING ORGANIZATION REPORT NUMBER
The MITRE Corporation JASON Program Office 7515 Colshire Drive McLean, Virginia 22102	JSR-08-531

9. SPONSORING / MONITORING AGENCY NAME(S) AND ADDRESS(ES)	10. SPONSOR/MONITOR'S ACRONYM(S)
Center for Security Evaluation 2100 K. Street, Suite 500 Washington, DC 20427-001	11. SPONSOR/MONITOR'S REPORT NUMBER(S)

12. DISTRIBUTION / AVAILABILITY STATEMENT

Approved for public release; distribution unlimited.

13. SUPPLEMENTARY NOTES

14. ABSTRACT

This note derives the distribution of electrical spreading currents along the length of solid conducting objects for which the length substantially exceeds the width. Sources and sinks of DC (or very low frequency AC) current are placed at one end of the object, and the fall-off of spreading current is studied as a function of length. The fall-off can be great; for instance in the case of a solid rectangular object, the fall-off of spreading current along the length is 27dB per unit width. Comparison is made to inductive coupling, which becomes important as frequency increases.

15. SUBJECT TERMS

16. SECURITY CLASSIFICATION OF:			17. LIMITATION OF ABSTRACT	18. NUMBER OF PAGES	19a. NAME OF RESPONSIBLE PERSON
					Brian O'Connor
a. REPORT	b. ABSTRACT	c. THIS PAGE	UL		19b. TELEPHONE NUMBER (include area code) 202-496-5144
Uncl	Uncl	Uncl			

Current Spreading in Long Objects

October 2008

JSR-08-531

Contact: D. McMorrow - dmcmorrow@mitre.org

Contents

Abstract

This note derives the distribution of electrical spreading currents along the length of solid conducting objects for which the length substantially exceeds the width. Sources and sinks of DC (or very low frequency AC) current are placed at one end of the object, and the fall-off of spreading current is studied as a function of length. The fall-off can be great; for instance in the case of a solid rectangular object, the fall-off of spreading current along the length is 27dB per unit width. Comparison is made to inductive coupling, which becomes important as frequency increases.

1 INTRODUCTION

When we inject a current into a solid conducting body at one point on its surface, and allow the current to flow back out at another point, the current distribution within the body spreads out around the direct path from source to sink. This is called "current spreading", and is important in semiconductor design, where crosstalk among different devices on the same chip must be minimized [1].

In this note we are particularly interested in the decay of DC current spreading along the length of a long conducting body when both source and sink are at one end. We will find that the magnitude of spreading current generally falls off like $\exp(-kz)$, where z is the distance away from the current source along the long axis of the body, and k is a characteristic decay coefficient.

In the language of electrical engineering, we drive the body as a (poor!) transmission line with DC in differential mode at one end, and measure the decay along the distance z as some number of dB per unit length,

$$K \equiv 20 \log_{10}(e)k \quad \text{dB/length}. \tag{1-1}$$

Note that k is independent of the resistivity of the material (as long as the body is uniform in composition); it depends only on geometry of the body. The current source is assumed to supply the necessary voltage to drive the current; the decay is due to geometrical effects on the current distribution, as it wends its way through the resistive material. Experimentally, we can measure the fall-off of voltage $V(z)$ over a cross-section of the body, as a function of distance z in the long direction of the body; see Figure 1. In fact this measurement would be easy to do and is strongly recommended for any practical applications.
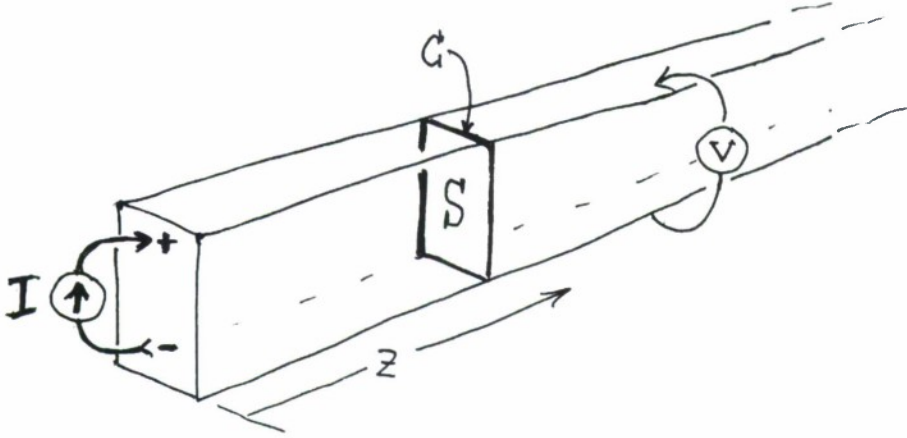
1

Figure 1: Measurement of current spreading for a long object. We inject a known current in differential mode at the end of the semi-infinite object. We then measure voltages $V(z)$ across the object at various distances z in the long dimension. The body has cross-section S bounded by curve C.

At DC, the only important length scale is the cross-section size. For AC at all but the lowest frequencies, another length scale becomes important, namely the skin depth; and inductive effects will become important too. We begin by studying the DC problem. Finite-frequency effects including skin depth and induction will be briefly discussed in Section 4.

2   DC EQUATIONS AND THEIR SOLUTION

We use cartesian coordinates (x, y, z) and model our solid body as a right cylinder with long axis along z. The cross-section of the body is a region S in the (x, y) plane bounded by a curve C, and is constant in z. One end of the body lies in the plane $z = 0$, and the body extends over $0 \leq z < \infty$, and so is half-infinite.

Hollow cylindrical bodies can be equally well modelled by using a curve C which consists of two (or more) separated components, one inside the other. A pair of separate conducting bodies could be modelled by a cross-section S consisting of two separate disconnected components; however we will take S to be connected unless otherwise specified.

The body is composed of material of some constant resistivity σ. We study the stationary Maxwell equations [2] in which all time derivatives are neglected, and so all fields, and the current, will be functions of (x, y, z) but not time t.[1] Steady electrical current flow within the body is described by the current density $\vec{\mathbf{J}}$ and obeys the equations

$$\vec{\nabla} \cdot \vec{\mathbf{J}} = 0, \quad \vec{\mathbf{J}} = \sigma \vec{\mathbf{E}} \qquad (2\text{-}1)$$

where $\vec{\mathbf{E}}$ is the electric field. On the sides of the cylinder no current flows across the surface, so the boundary condition is

$$\hat{\mathbf{n}} \cdot \vec{\mathbf{J}} = 0 \quad \text{on } C \text{ for all } z \geq 0 \qquad (2\text{-}2)$$

where $\hat{\mathbf{n}}$ is the unit normal to C in any plane $z = \text{const}$. On the end $z = 0$ of the cylinder we impose some source J_0 of injected and sunk currents,

$$\hat{\mathbf{z}} \cdot \vec{\mathbf{J}} = J_0(x, y) \quad \text{at } z = 0. \qquad (2\text{-}3)$$

---

[1]In this section, frequency is DC, or so low that inductive effects can be neglected; for the latter see Section 4.

The electric field can be expressed in term of the gradient of the electostatic potential Φ,

$$\vec{E} = -\vec{\nabla}\Phi \qquad (2\text{-}4)$$

and eliminating both $\vec{E}$ and $\vec{J}$ from Eqs. (3.2,3.5) we obtain equations determining Φ as

$$\nabla^2\Phi \;=\; 0 \quad \text{inside the body} \qquad (2\text{-}5)$$

$$\hat{\mathbf{n}} \cdot \vec{\nabla}\Phi \;=\; 0 \quad \text{on } C \text{ for all } z \geq 0 \qquad (2\text{-}6)$$

$$\frac{\partial \Phi}{\partial z} \;=\; -\sigma^{-1} S(x,y) \quad \text{at } z = 0 \qquad (2\text{-}7)$$

which describe a well posed boundary value problem with Neumann boundary conditions. (For notation and methods see, *e.g.*, [2]).

This problem can be solved by separation of variables,

$$\Phi(x,y,z) \;=\; \psi(x,y)f(z) \qquad (2\text{-}8)$$

$$\nabla_t^2 \psi(x,y) + k^2 \psi(x,y) \;=\; 0 \qquad (2\text{-}9)$$

$$\hat{\mathbf{n}} \cdot \vec{\nabla}\psi \;=\; 0 \quad \text{on } C \qquad (2\text{-}10)$$

$$\frac{\partial^2 f(z)}{\partial z^2} \;=\; -k^2 f(z) \qquad (2\text{-}11)$$

with corresponding boundary conditions at $z = 0$, see below, where $k \geq 0$ is a separation constant, and where the Laplacian operator in the (x,y) plane is

$$\nabla_t^2 = \frac{\partial^2}{\partial x^2} + \frac{\partial^2}{\partial y^2} \; . \qquad (2\text{-}12)$$

We can form any solution Φ by use of the eigenfunctions of the transverse Neumann boundary value problem,

$$\nabla_t^2 \psi_i(x,y) = -\lambda_i \psi_i(x,y), \quad \hat{\mathbf{n}} \cdot \vec{\nabla}\psi = 0 \quad \text{on } C \qquad (2\text{-}13)$$

with eigenvalues $\lambda_i, i = 0,1,2\ldots$ by means of the expansion

$$\Phi(x,y,z) = \sum_{i=0}^{\infty} c_i \psi_i(x,y) \exp(-k_i z) \qquad (2\text{-}14)$$

4

where $\lambda_i = k_i^2$. The eigenvalues λ_i will be assumed ordered by nondecreasing value, and the eigenfunctions $\psi(x, y)$ will be normalized to unity in the L_2 norm.

For any body the lowest eigenvalue and its eigenfunction are always

$$\lambda_0 \;=\; 0 \tag{2-15}$$

$$\psi_0 \;=\; c_1 \quad (c_1 \text{ is a normalizaton constant}) \tag{2-16}$$

which corresponds to uniform current injection into the end of the body with no current sink; such a current has $k_0 = 0$ and therefore is constant in the z-direction; it represents common-mode current flow through the body to $z = \infty$.

Since we are interested in differential mode current injection we will henceforth assume that $c_0 = 0$; then the decay of the spreading current in z is controlled by the next lowest eigenvalue $\lambda_1 > 0$.

$$k_1 \;=\; \sqrt{\lambda_1}, \tag{2-17}$$

$$K \;=\; (8.69\,\text{dB})k_1. \tag{2-18}$$

3 RESULTS FOR BODIES OF VARIOUS SHAPES

Example 1) The body is a solid rectangular object, so the cross-section S is a solid rectangle of dimensions d by w in the x and y directions respectively (with $d \geq w$). Then

$$\psi_1 = c_1 \cos(\pi x/d) \quad \text{independent of } y \tag{3-1}$$

$$\lambda_1 = (\pi/d)^2 \tag{3-2}$$

$$k_1 = \pi/d \tag{3-3}$$

$$K = 27 \, \text{dB}/d. \tag{3-4}$$

This result shows a remarkably fast fall-off K. For instance, to achieve an 80 dB fall-off, we need only go in the long direction three times the width.

Example 2) The body is a hollow rectangular box, so the cross-section S is a hollow square of dimensions d by w in the x and y directions respectively (with $d \geq w$), and with some small wall-thickness t. Then to a good approximation

$$\psi_1 = c_1 \cos(\pi p/(d+w)) \; (p \text{ is distance along the perimeter}) \tag{3-5}$$

$$\lambda_1 = (\pi/(d+w))^2 \tag{3-6}$$

$$k_1 = \pi/(d+w) \tag{3-7}$$

$$K = 27 \, \text{dB}/(d+w) \tag{3-8}$$

independent of t when $t \ll w$.

Example 3) The body is hollow and has a thin-walled cross-section of any shape, with P the total perimeter, that is, the length of C. Then

$$k_1 = 2\pi/P \tag{3-9}$$

$$K = 54 \, \text{dB}/P, \tag{3-10}$$

approximately independently of the wall-thickness $t \ll P$

Example 4) The body is a solid circular cylinder, so the cross-section S is a solid disk of diameter d. Then eigenfunctions are constructed out of Bessel functions $J_n(r)$ and angular functions $\exp(im\phi)$, and

$$\psi_1 \; = \; c_1 \, J_1(k_1 r) \exp(i\phi) \quad (r \text{ and } \phi \text{ are polar coordinates}) \qquad (3\text{-}11)$$

$$\lambda_1 \; = \; 4(x_{10}'^2 + 1^2)/d^2 \quad (x_{10}' \text{ is the first root of } J_1') \qquad (3\text{-}12)$$

$$k_1 \; = \; 4.19/d \qquad (3\text{-}13)$$

$$K \; = \; 36 \, \text{dB}/d. \qquad (3\text{-}14)$$

Example 5) The body is an "I-beam", so the cross-section is a letter "I" with depth d (in the y-direction), width w ($< d$) (in the x-direction), and small thickness t. Then a good approximation is

$$\psi_1 \; = \; c_1 \, \cos(\pi y/d) \quad \text{independent of } x \qquad (3\text{-}15)$$

$$\lambda_1 \; = \; (\pi/d)^2 \qquad (3\text{-}16)$$

$$k_1 \; = \; \pi/d \qquad (3\text{-}17)$$

$$K \; = \; 27 \, \text{dB}/d. \qquad (3\text{-}18)$$

These examples are summarized in Figure 2.

Example 6 We now turn to bodies constructed of discrete components, such as lattices of metal struts. To model these bodies we employ infinite ladders of resistors, as shown for example in Figure 3(a). Each stage consists of one transverse resistor (a "rung") R_1, and two longitudinal resistors (the "stringers") R_2. To compute the properties of such a ladder, use a well-known trick shown in Figure 3(b): The unknown effective resistance R_X looking into the end the ladder can be determined by observing that adding one more stage to the ladder, leaves it invariant, so
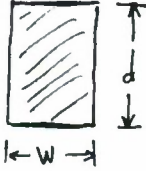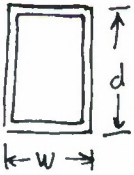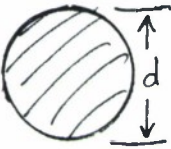
$$1/R_X = 1/R_1 + 1/(R_X + 2R_2), \qquad (3\text{-}19)$$
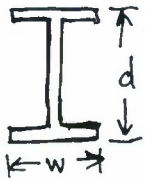
8

1) solid rectangular cross section $K = 27\ dB/d$

2) hollow rectangle (+thin wall) $K = 27\ dB/(d+w)$

3) any hollow body (+thin wall) $K = 54\ dB/P$

4) solid circle $K = 36\ dB/d$

5) "I-beam" $K = 27\ dB/d$

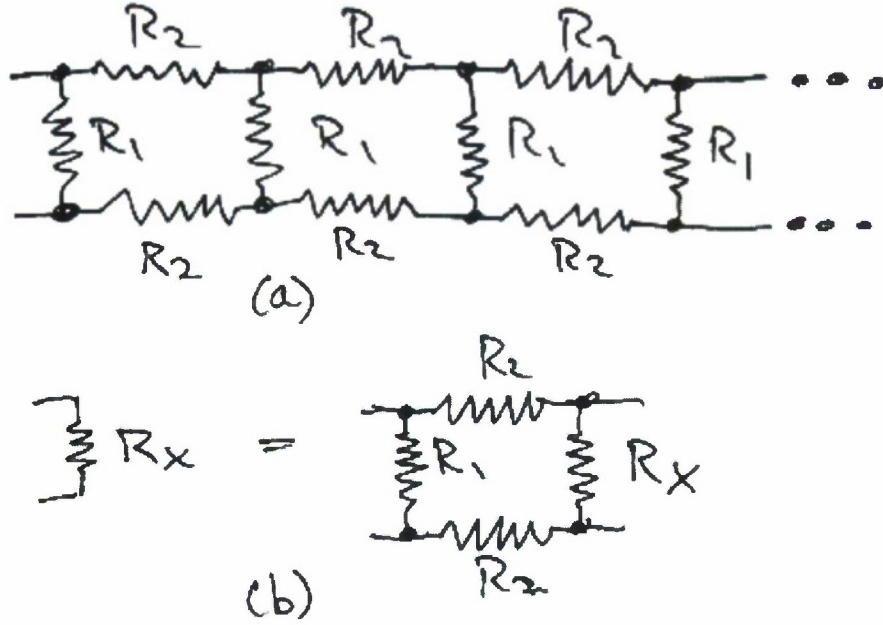Figure 2: Cross sections, dimensions and values of K for the examples.

Figure 3: (a) A semi-infinite resistor ladder. All transverse resistors are R_1. All longitudinal resistors are R_2. (b) The effective resistance R_X looking into the ladder, which can be determined by adding one stage, which gives the same R_X.

which is readily solved for R_X as

$$R_X = -R_2 + \sqrt{R_2^2 + 2R_1 R_2} \tag{3-20}$$

For instance, if all resistors are equal, $R_1 = R_2$, the fall-off is readily shown to be

$$K = 11\,\mathrm{dB/stage} \quad \text{ladder of equal resistors} . \tag{3-21}$$

To achieve higher values of K we can subdivide the R_2's and add more rungs R_1 for a total of N rungs per stage, which we model with $R_2 = R_1/N$. We compute

10

N	K
1	11 dB/stage
2	17 dB/stage
3	21 dB/stage
4	24 dB/stage
5	27 dB/stage
10	39 dB/stage

These results show that adding more "rungs" increases the fall-off substantially.

Example 7 We now turn to 3-dimensional resistor ladders, as in Figure 4(a). Each stage consists of four transverse resistors R_1, and four longitudinal resistors R_2. How shall we compute this? The "ladder trick" does generalize, but becomes cumbersome. A faster computation goes as follows. The ladder shows a four-fold rotational symmetry when we look along it from its end, so the eigenfunctions of current distribution must be proportional to $\exp(im\phi)$ for $m = (0, 1, 2)$ where ϕ is angle about the long axis; see Figure 4(b,c,d). As can be expected, the $m = 0$ mode is common-mode current flow along the ladder to infinity, and can be ignored. The next-lowest modes are the two $m = 1$ modes, which are degenerate, shown in Figure 4(c). However, in these modes, half the transverse resistors R_1 carry no current because the voltage across them vanishes by symmetry. Therefore half of all the resistors R_1 can be chopped out, and the box decomposes into two 2-dimensional ladders as in Example 6). Therefore all the values of K are exactly the same as found above for Example 6).

Again, these examples apply at frequencies so low that inductive effects can be neglected. What happens at higher frequency?
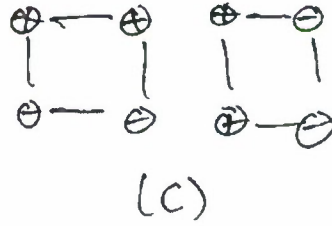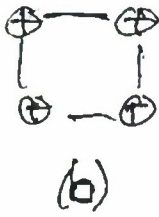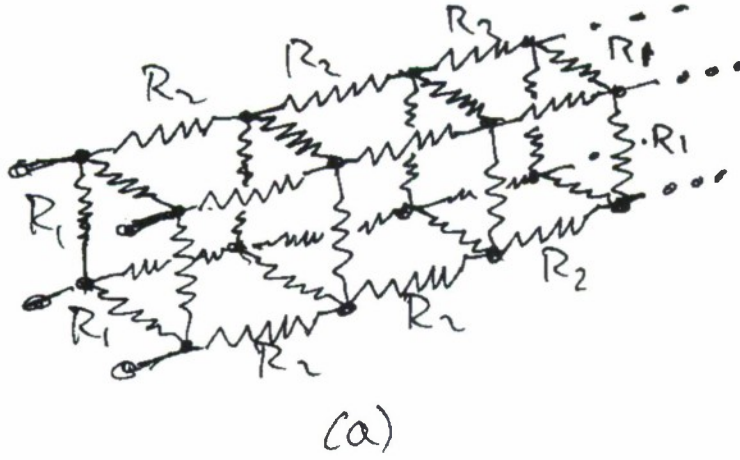
11

Figure 4: (a) A more elaborate semi-infinite resistor ladder, with a box-like stage. All transverse resistors are R_1. All longitudinal resistors are R_2. (b,c,d) The symmetries of the normal modes of this ladder are like $\exp(im\phi)$ with $m = (0, 1, 2)$ respectively.

4 FINITE-FREQUENCY EFFECTS: INDUCTION

As frequency ω is raised, the first effect to become important is induction of electomotive force (EMF) by the time-dependent magnetic field $\vec{\mathbf{B}}$ (while charge separation, and displacement current associated with time-dependent $\vec{\mathbf{E}}$ are still negligible). Maxwell's equations can then be written [2]

$$\vec{\nabla} \cdot \vec{\mathbf{J}} = 0, \qquad \vec{\mathbf{J}} = \sigma\vec{\mathbf{E}} \tag{4-1}$$

$$\nabla \times \vec{\mathbf{B}} = \mu\vec{\mathbf{J}} \tag{4-2}$$

$$\nabla \times \vec{\mathbf{E}} = -\partial\vec{\mathbf{B}}/\partial t \quad \text{(induction equation)} \tag{4-3}$$

$$\vec{\mathbf{E}} = -\vec{\nabla}\Phi - \partial\vec{\mathbf{A}}/\partial t \tag{4-4}$$

$$\vec{\mathbf{B}} = \nabla \times \vec{\mathbf{A}} \tag{4-5}$$

$$\text{where} \tag{4-6}$$

$$\vec{\mathbf{A}} = \text{vector potential with } \nabla \cdot \vec{\mathbf{A}} = 0. \tag{4-7}$$

Here, all fields depend on time like $\exp(-i\omega t)$, and moreover depend on spatial coordinates (x, y, z); μ is the magnetic permeability of the material. Eliminating $\vec{\mathbf{E}}$, $\vec{\mathbf{B}}$ and $\vec{\mathbf{J}}$ leads to a Laplace equation for Φ, and a diffusion equation for $\vec{\mathbf{A}}$

$$\nabla^2\Phi = 0 \tag{4-8}$$

$$\nabla^2\vec{\mathbf{A}} + i\mu\sigma\omega\vec{\mathbf{A}} = -\mu\sigma\nabla\Phi. \tag{4-9}$$

The "skin effect" is one important effect governed by these equations: current tends to concentrate near the surface of a conducting body, in a layer of thickness roughly

$$\delta = \sqrt{2/\mu\sigma\omega} \quad \text{"skin depth"} \tag{4-10}$$

with fields and currents falling off like $\exp(-d/\delta)$ with distance d from the surface. When this is the main effect at finite frequency, we expect Eq. (3-10) above to still apply approximately, with the "body" replaced by a thin shell of thickness $t \sim \delta$. To estimate the effect, recall that skin depth is of order a few cm in common metals at 60Hz, except that it may be much less due to permeability of ferromagnetic materials. Thus for frequencies of 60Hz and higher, the thin-shell approximation Eq. (3-10) applies.

However a different effect may be much more important. Unlike currents, magnetic fields can traverse free space *outside* the body; different parts of the body can therefore be coupled by mutual inductance. This coupling can be expected to fall off, not exponentially, but as a power-law of distance z. (This is because the exciting current generally has some magnetic ℓ-pole moment, and the magnetic field falls off like $(\text{distance})^{-\ell-2}$ from it. Technically, the equation for $\vec{\mathbf{A}}$ has an unbounded domain, and therefore has a continuous spectrum of eigenvalues.)

Let us estimate the inductive effect of finite frequency f in a rectangular body of cross-section $d \times w$ as above. If the current source has a magnetic dipole moment $\sim I d^2$, then the electric field induced by the time-changing magnetic field propagating through free space is roughly

$$E_{\text{induct}} \sim \frac{\omega \mu_0 I d^2}{8 z^2} \tag{4-11}$$

where $\omega = 2\pi f$ is the angular frequency and μ_0 is the constant permeability of free space (and we take the material as not strongly magnetic). This must be compared with the conductive electric field inside the material

$$E_{\text{conduct}} \sim \frac{I}{\sigma dw} \exp(-kz) \, . \tag{4-12}$$

Their ratio is

$$\frac{E_{\text{induct}}}{E_{\text{conduct}}} \sim \frac{dw}{\delta^2} \cdot \frac{\exp(kz) d^2}{z^2} \, . \tag{4-13}$$

14

where Eq. (4-10) has been used to eliminate ω. So in this example, inductive effects dominate spreading current at modest values of z, when δ is no larger than the transverse size. In a hollow body (or "I-beam") of thickness t, the corresponding expression is

$$\frac{E_{\text{induct}}}{E_{\text{conduct}}} \sim \frac{dt}{\delta^2} \cdot \frac{\exp(kz)d^2}{z^2} \tag{4-14}$$

and inductive effects will certainly dominate when $\delta < t$.

For a discrete ladder (as in Examples 6 and 7 above), one significant effect is that each component now has a combination of resistive and self-inductive impedance. When this is the main effect of finite frequency, we still find exponential decay of currents along the ladder, and K can computed in just the same way.[2]

However, once again, mutual inductance is likely to dominate. The mutual inductance of distant discrete elements generally falls off as a power-law in stage number along the ladder, not as an exponential, and is likely to dominate at long distances.

For both continuous and discrete bodies, the important effect at high enough frequency is therefore likely to be the inductive coupling of distant elements, which would have to be computed by different methods than developed in this note. At yet higher frequencies, charge separation and capacitive coupling will eventually become important too. Finally, at RF frequencies, displacement current becomes important, giving radiative effects.

---

[2]K now has an imaginary part which describes an uninteresting phase shift along the ladder.

5 CONCLUSIONS

We have shown how to compute the fall-off of spreading current in long conducting objects, for differential-mode DC current injection at one end. We have also computed a variety of examples. The results show that the fall-off is remarkably fast in many examples. Practical applications are recommended when the control of spreading currents is desirable. AC current spreading will differ due to inductive effects, and must also be carefully assessed.

6 ACKNOWLEDGEMENTS

References

[1] Simon M. Sze & Kwok K. Ng, *Physics of Semiconductor Devices*, Wiley-Interscience, New York, 2006.

[2] J. David Jackson, *Classical Electrodynamics*, Wiley, New York, 1999.

DISTRIBUTION LIST

Assistant Secretary of the Navy
(Research, Development & Acquisition)
1000 Navy Pentagon
Washington, DC 20350-1000

Assistant Deputy Administrator for
Military Application
NA-12
National Nuclear Security Administration
U.S. Department of Energy
1000 Independence Avenue, SW
Washington, DC 20585

DARPA Library
3701 North Fairfax Drive
Arlington, VA 22203-1714

Director of Space and SDI Programs
SAF/AQSC
1060 Air Force Pentagon
Washington, DC 20330-1060

Deputy Under Secretary of
Defense Science & Technology
3040 Defense Pentagon
Washington, DC 20301-3040

Defense Technical Information Center (DTIC)
8725 John J. Kingman Road
ATTN: DTIC-OA (Mr. Jack Rike)
Suite 0944
Fort Belvoir, VA 22060-6218

Director, DTRA
Research Development Office
8725 John Jay Kingman Road
Rm 3380, Mail Stop 6201
Fort Belvoir, VA 22060

Headquarters Air Force XON
4A870 1480 Air Force Pentagon
Washington, DC 20330-1480

IC JASON Program [2]
Chief Technical Officer/OCS
2P0104 NHB
Central Intelligence Agency
Washington, DC 20505-0001

JASON Library [5]
The MITRE Corporation
3550 General Atomics Court
Building 29
San Diego, CA 92121-1122

Records Resource
The MITRE Corporation
Mail Stop D460
202 Burlington Road, Rte 62
Bedford, MA 01730-1420

Reports Collection
Los Alamos National Laboratory
Mail Station 5000
MS A150
PO Box 1663
Los Alamos, NM 87545

Superintendent
Code 1424
Attn: Documents Librarian
Naval Postgraduate School
Monterey, CA 93943

U S Army Space & Missile Defense Command
Attn: SMDC-ZD (Dr. Swinson)
PO Box 1500
Huntsville, AL 35807-38017

Administrator
U.S. Dept of Energy
National Nuclear Security Administration
1000 Independence Avenue, SW
NA-10 FORS Bldg
Washington, DC 20585

Principal Deputy Director
Office of Science, SC-2/Forrestal Building
U.S. Department of Energy
1000 Independence Avenue, SW
Washington, DC 20585

Director
Institute for Defense Analyses
Technical Information Services
Room 8701
4850 Mark Center Drive
Alexandria, VA 22311-1882

Dr. Lawrence K. Gershwin
NIC/NIO/S&T
2E42, OHB
Washington, DC 20505

Dr. Alfred Grasso
President & CEO
The MITRE Corporation
Mail Stop N640
7515 Colshire Drive
McLean, VA 22102-7508

Dr. Barry Hannah
Reentry Systems Branch Head, Navy Strategic
Systems Programs
Strategic Systems Programs (Attn: SP28)
2521 Clark Street, Suite 1000
Arlington, VA 22202-3930

Dr. Robert G. Henderson
The MITRE Corporation
Mailstop MDA/ Rm 5H305
7515 Colshire Drive
McLean, VA 22102-7508

Dr. Bobby R. Junker
Office of Naval Research
Code 31
800 North Quincy Street
Arlington, VA 22217-5660

Mr. Kevin "Spanky" Kirsch
Director, Special Programs
US Department of Homeland Security
Science and Technology Directorate
Washington, DC 20528

Dr. Daniel J. McMorrow
Director, JASON Program Office
MITRE Corporation
Mailstop T130
7515 Colshire Drive
McLean, VA 22102-7508

Dr. Julian C. Nall
Institute for Defense Analyses
4850 Mark Center Drive
Alexandria, VA 22311-1882

Deputy Chief Scientist
U.S. Army Space & Missile Defense Command
PO Box 15280
Arlington, VA 22215-0280

Dr. John R. Phillips
Chief Scientist, DST/CS
2P0104 NHB
Central Intelligence Agency
Washington, DC 20505-0001

Dr. William S. Rees, Jr.
OSD/DDR&E
Deputy Under Secretary of Defense for
Laboratories and Basic Sciences
3030 Defense Pentagon
Room 3C913A
Washington, DC 20301-3030

Mr. Alan R. Shaffer
Principal Deputy Director
DDR&E
3040 Defense Pentagon, Room 3B 854
Washington, DC 20301-3040

Mr. Anthony J. Tether
DIRO/DARPA
3701 N. Fairfax Drive
Arlington, VA 22203-1714